EFFECTS OF ANNEALING TEMPERATURE ON OPTICAL AND ELECTROCHEMICAL PROPERTIES OF SPRAY-PYROLYSED WO_3 FILMS

Mono Zaw[1], Aung Chan Thar[2], Nyein Wint Lwin[3] and Than Zaw Oo[4]

Abstract

Tungsten trioxide (WO_3) thin films were coated onto fluorine tin oxide (FTO) coated glass substrates by spray pyrolysis technique and annealing at different temperatures (300ºC, 400ºC and 500ºC). The presented work studied the effect of annealing temperature on the surface morphology, optical and electrochemical properties of WO_3 films by using scanning electron microscopy (SEM), atomic force microscopy (AFM), UV-vis spectroscopy and cyclic voltammetry (CV). Optical study showed that the decreased optical transmission and band gap was observed in WO_3 film at higher annealing temperature (400ºC and 500ºC). The electrochemical study revealed that anodic peak current density was higher in WO_3 film annealed at 400ºC in KI electrolytic solution. Upon modulating the annealing temperature, change in optical and electrochemical properties of WO_3 films was correlated to surface morphology change in WO_3 films.

Keywords: Optical properties, Tungsten trioxide film, Annealing temperature, Electrochromism

Introduction

Electrochromic (EC) materials and devices are reversible change in color, or optical density, with a change in voltage or electric potential [Ruyu H.Y. *et al*., J. Materials Science, **39** (2004) 4377].

The important feature of electrochromic glass is the ability to response toward the apply voltage in shortest time and endurance to maintain in color shape after apply voltage. A lot of attention has been devoted in the latter application due to the potential for significant energy saving by reducing cooling and heating loads and a better management of the natural light [Rajeshwar A.W. *et al*., J. Electroanalytical Chemistry, **612** (2008) 112]. The application of the electrochromic smart glass include anti-glare automobile rearview mirrors, sun-roofs, electronic shutters, hydrogen sensors, displays and energy efficient "smart" windows [Gilliaspie D.T. *et al*., J. Materials Chemistry, **20** (2010) 9585]. They can be built in a form of electrochromic device with one or two electrochemically active coatings that change color during an oxidation-reduction process.

Electrochromic (EC) devices can be made from organic and inorganic materials. The advantage of inorganic materials based electrochromic device is that they are much more stable in sunlight and have longer lifetime. Transition metal oxides (inorganic materials) such as tungsten trioxide (WO_3), nickel oxide (NiO), molybdenum trioxide (MoO_3) and iridium trioxide (IrO_3) have been widely used in electrochromic materials. The electrochromic (EC) materials change their optical properties when charge insertion or extraction and this may cause the material change its color. Materials that change color upon charge insertion are called cathodic while materials that change color upon charge extraction are called anodic. Oxides of Tungsten (W), Titanium (Ti) and Molybdenum (Mo) exhibit cathodic electrochromism and oxides of Vanadium (V), Nickel (Ni) and Iridium (Ir) exhibit anodic electrochromism. [Niklasson G.A. *et al.*, J. Materials Chemistry, **17** (2007) 127]

[1] Assistant Lecturer, Department of Physics, University of Mandalay, Mandalay, Myanmar
[2] Dr, Lecturer, Department of Physics, Mohyin Degree Collage, Kachin, Myanmar
[3] Dr, Professor, Department of Physics, University of Mandalay, Mandalay, Myanmar
[4] Dr, Professor, Universities' Research Centre, University of Yangon, Yangon, Myanmar

Tungsten trioxide (WO_3) is the most studied among the electrochromic materials and exhibits an n-type semiconducting behavior with a band gap energy of 2.5-3.3 eV [Jayachandran M. *et al*., Transactions of the SAEST. **40** (2005) 42]. There are various choices for preparing WO_3 films with the development of thin film technology. These include sputtering, chemical vapor deposition, spray pyrolysis, evaporation, sol-gel and laser ablation deposition. Among these, spray pyrolysis method is the most cost-effective for producing large-area films, and enables a better control over the film growth and hence more homogenous and more transparent films are yielded [Daniel M.F. *et al*., J. Solid State Chemistry, **67** (1987) 235.]

Materials and Methods

Tungsten trioxide (WO_3) powder (0.05 M) was dissolved in 50 ml of ammonia at 80^oC under continuous stirring for 30 min to form tungsten trioxide (WO_3) precursor solution. The obtained WO_3 solution was diluted with 10 ml of deionized water and then cooled down to room temperature and filtered. After that, the final WO_3 solution was sprayed on the FTO substrate (substrate temperature is 300^oC) by using spray pyrolysis method to obtain WO_3 films. The resulting WO_3 films with the WO_3 concentration of 0.05 M were annealed at different temperatures (300^oC, 400^oC and 500^oC) for 1 hour.

The surface feature of WO_3 films was measured by scanning electron microscopy (SEM) and atomic force microscopy (Nanosurf Naio AFM). The optical properties of WO_3 films were performed using UV-vis spectrophotometry (Genesys 10S). The electrochemical properties of WO_3 films were characterized by cyclic voltammetry (CV) (Electrochemical Workstation-CorrTest CS350).

Results and Discussion

3.1 Surface morphology of WO_3 Films

The surface morphology of WO_3 films was examined by Scanning Electron Microscopy (SEM) and Atomic Force Microscopy (AFM). Figure 3.1 (a-c) shows the SEM micrograph of WO_3 films for different annealing temperatures in two dimensional view. From the SEM micrograph, the surface feature of WO_3 films annealed at 300^oC reveals the cracking surface. This cracking is formed so many gap on the WO_3 films. The surface morphology of WO_3 films for 400^oC and 500^oC are relatively the same with a rough surface and uniformly covered. In addition, the solvent evaporation can cause defects in the surface, such as pores, cracks etc. Moreover, the surface morphology of WO_3 films was shown with three dimensional view by AFM technique. Figure 3.2 (a-c) shows the AFM micrograph of WO_3 films for different annealing temperatures. Like the case of SEM results, the surface morphology of WO_3 thin films annealed at 400^oC shows better surface conformation rather than that of other WO_3 samples. It may provide the better performance of electrochromic device.

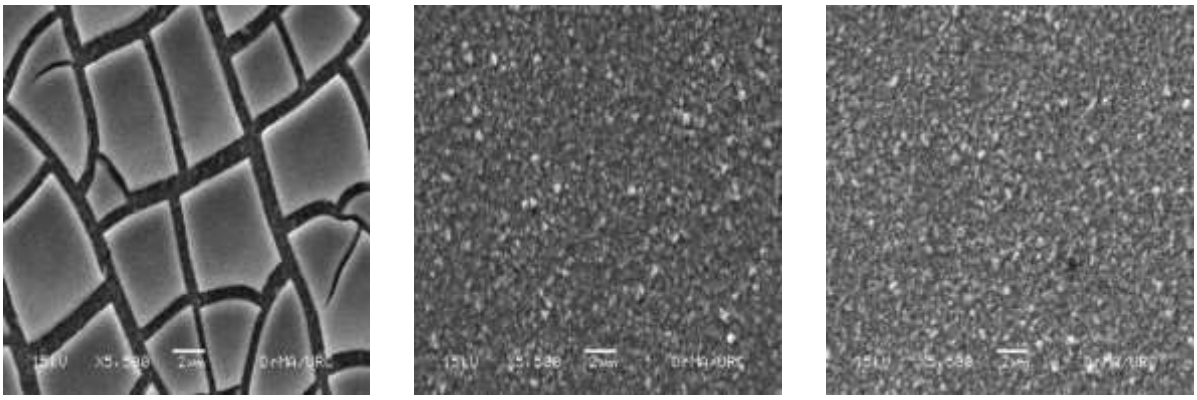

(a) (b) (c)

Figure 3.1 SEM micrograph of WO_3 films with different annealing temperatures (a) 300°C, (b) 400°C and (c) 500°C

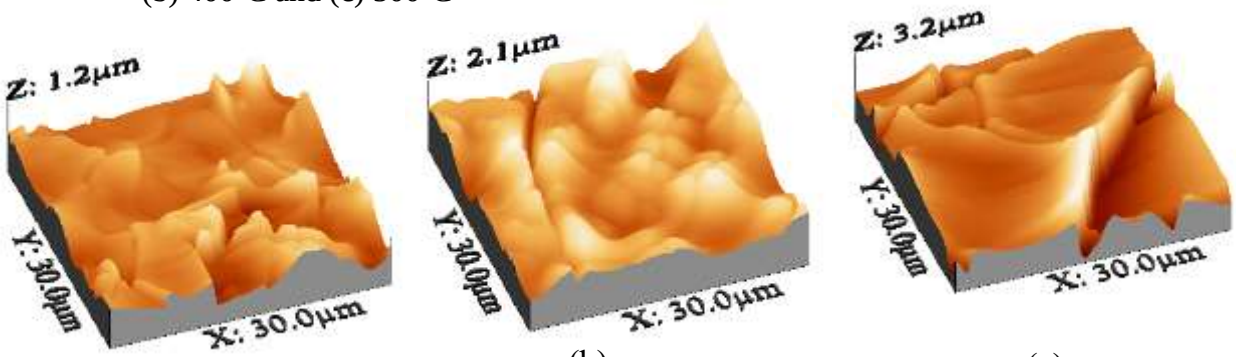

(a) (b) (c)

Figure 3.2 AFM micrograph of WO_3 films with different annealing temperatures (a) 300°C, (b) 400°C and (c) 500°C

3.2 Optical Transmission and Band Gap Energy of WO_3 Films

The optical properties of WO_3 films were investigated varying with annealing temperatures. The optical transmission spectra of WO_3 films were measured by UV- vis spectrophotometry. The optical transmission spectra of WO_3 films with different annealing temperatures are depicted in Figure 3.3 (a). From this figure, the values of the optical transmission in the visible region are listed in Table 3.1. The highest optical transmission of WO_3 films is observed at 300°C. It may be due to the surface defects (larger number of holes and cracking) of WO_3 films. The optical transmission of WO_3 films for 400°C and 500°C are almost overlap in the visible region. Upon increasing annealing temperatures, the optical transmission of WO_3 films decreased. It is due to the fully coverage of the sample and better surface formation of WO_3 films. The optical transmission of WO_3 films decreased upon increasing annealing temperatures which is ascribed to the surface conformity of WO_3 films at higher annealing temperatures.

The optical band gap energy of WO_3 films was determined from Tauc's plot equation, $(\alpha h\nu)^n = A\,(h\nu - E_g)$, where α is absorption coefficient, $h\nu$ is incident light energy, and E_g is the band gap of the material. The exponent 'n' examine the transition type of the material. The value of n is 1/2 for indirect transition and is 2 for direct transition. The value of the optical band gap of WO_3 films was obtained by extrapolating the linear portion of the curve to photon energy axis. Figure 3.3 (b) shows the plot of the $(\alpha h\nu)^{1/2}$ versus $h\nu$ graph. The values of the band gap energy of

WO_3 films are listed in Table 3.1 for all annealing temperatures. The optical band gap energy values of WO_3 films decreased upon increasing annealing temperatures.

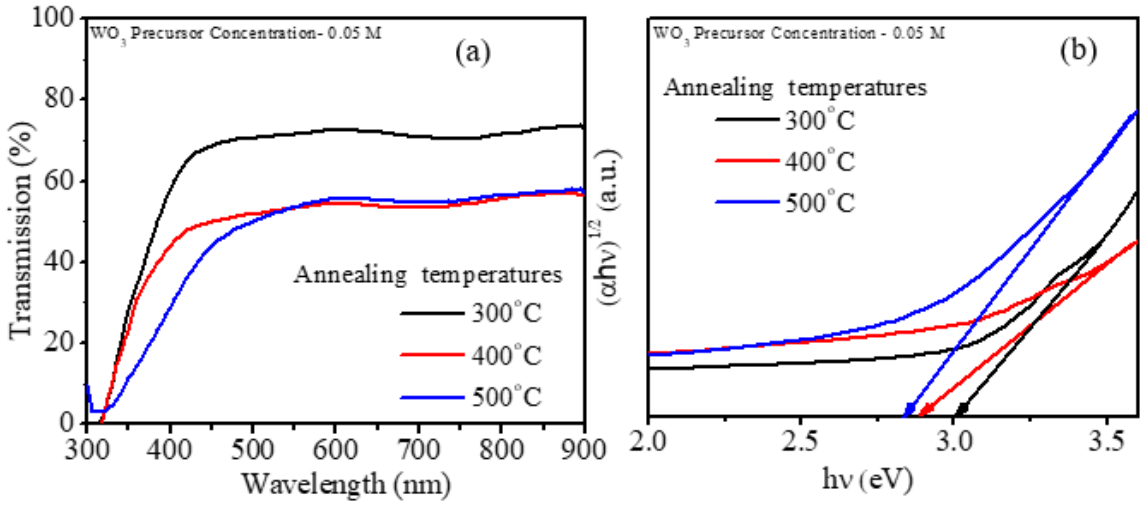

Figure 3.3 (a) Optical transmission spectra and (b) Plot of $(\alpha h\nu)^{1/2}$ versus $h\nu$ of WO_3 films with different annealing temperatures

Table 3.1 The value of optical transmission and band gap energy of WO_3 films with different annealing temperatures

Annealing Temperatures	Transmission (%)	Band gap energy (E_g) (eV)
300°C	75	3.0
400°C	50	2.9
500°C	55	2.7

3.3 Electrochemical Properties of WO_3 Films

Effect of annealing temperatures on electrochemical properties of WO_3 films were explored by cyclic voltammetry (CV). CV measurement is important for determining the performance of electrochromic device. Figure 3.4 (a-c) shows the CV graph of WO_3 films for all annealing temperatures with different scan rate in potassium iodide (KI) electrolytic solution. The cyclic voltammograms of WO_3 films were recorded in the potential range from – 0.4 V to + 0.2 V for each scan rate. The values of the anodic peak current density of WO_3 films for different annealing temperatures are obtained from the CV graph. As can be seen in the CV graph, the highest anodic peak current density of WO_3 films was observed at the annealing temperature 400°C for each scan rate. It is agreed with the earlier speculation of AFM results. The better surface homogeneity of WO_3 films annealed at 400°C gives the highest anodic peak current density for each scan rate. The values of the anodic peak current density of WO_3 films with different annealing temperatures are listed in Table 3.2. As can be seen in Figure 3.5, the highest anodic peak current density of WO_3 films was observed at the annealing temperature 400°C for different scan rates.

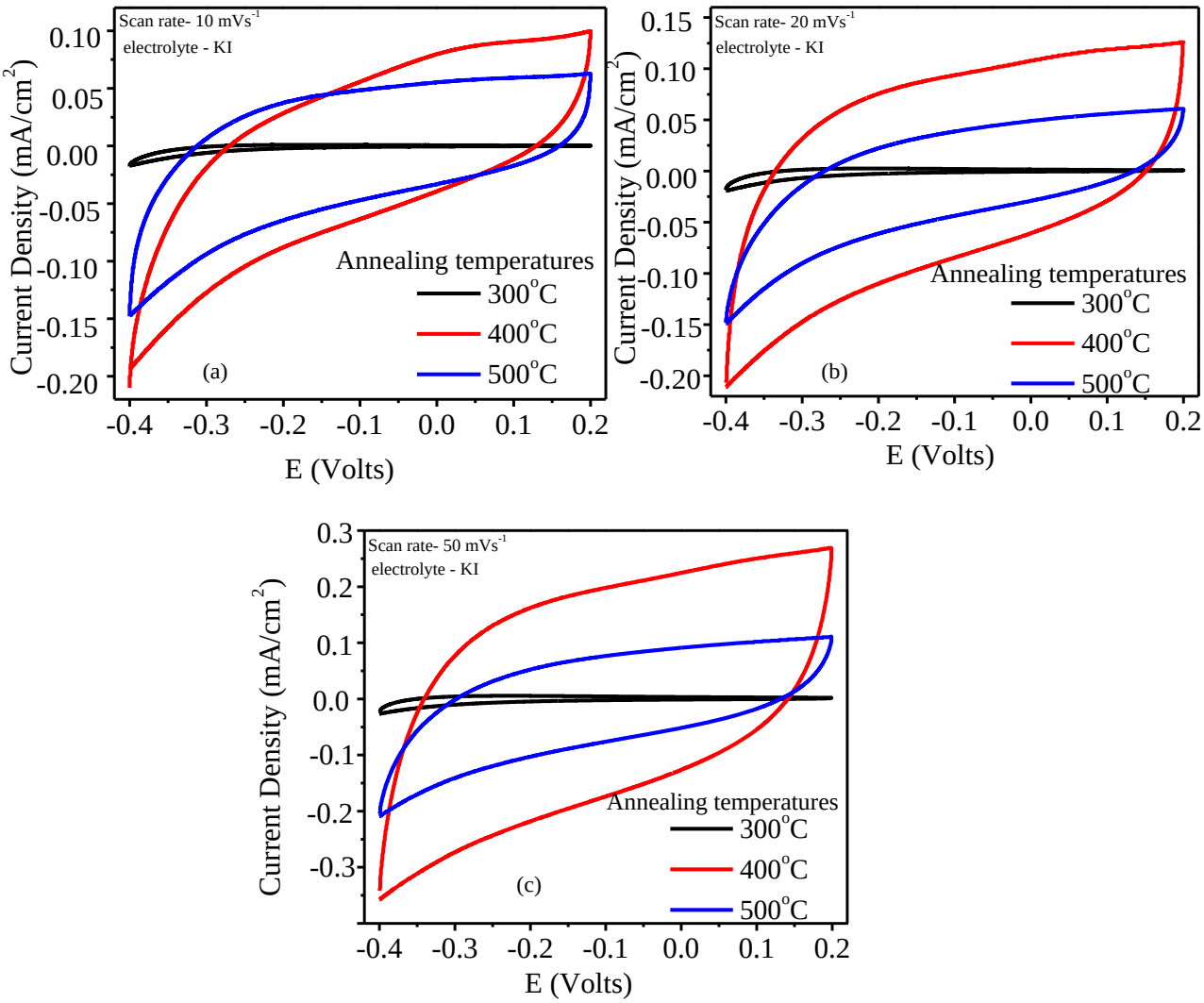

Figure 3.4 (a–c) Cyclic voltammogram of WO_3 films annealed at different temperatures (300°C, 400°C and 500°C) in KI electrolytic solution

Table 3.2 The values of anodic peak current densities of WO_3 films with different annealing temperatures in KI electrolytic solution

Scan Rate (mV/s)	Annealing Temperature	Anodic Peak Current Density (mA/cm^2)
10	300ºC	0.01
	400ºC	0.09
	500ºC	0.05
20	300ºC	0.01
	400ºC	0.12
	500ºC	0.06
50	300ºC	0.01
	400ºC	0.24
	500ºC	0.09

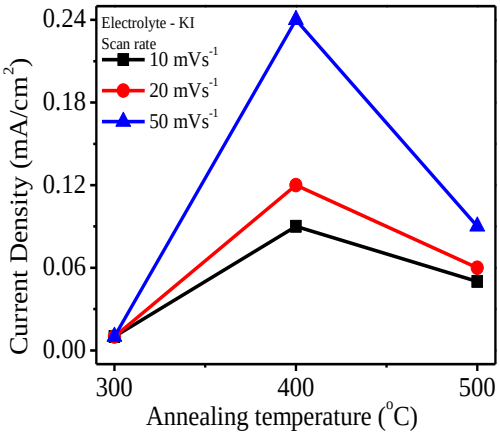

Figure 3.5 Plot of current density (mA/cm^2) Vs annealing temperature (^oC) of WO_3 films for all scan rates in KI electrolytic solution

Summary and Conclusion

Tungsten trioxide (WO_3) thin films were prepared from WO_3 aqueous solution by sol-gel method. The resulting WO_3 solution was transferred onto the substrate by spray pyrolysis method. The obtained WO_3 thin films were characterized by scanning electron microscopy (SEM), atomic force microscopy (AFM), UV-vis spectrophotometry and cyclic voltammetry (CV) by varying the annealing temperatures. The optical transmission and band gap energy of WO_3 films decreased upon increasing annealing temperatures. The electrochemical behavior of WO_3 films varying with annealing temperatures are tested by cyclic voltammetry (CV). The highest anodic peak current density of WO_3 films was observed at the annealing temperature 400°C for each scan rate in KI electrolytic solution. It may be due to the complete coverage of WO_3 thin films altered by annealing and it has sufficient colored species.

Acknowledgement

The authors special thanks to ISP (International Science Program), Sweden, for their support in measurement of cyclic voltammetry (Electrochemical Workstation- CorrTest CS350) and also grateful thank to all the Materials Science Laboratory members (University of Mandalay) for their helpful discussion.

References

Daniel M.F. *et al*., J. Solid State Chemistry, **67** (1987) 235.

Gilliaspie D.T. *et al*., J. Materials Chemistry, **20** (2010) 9585

Jayachandran M. *et al*., Transactions of the SAEST. **40** (2005) 42.

Niklasson G.A. *et al*., J. Materials Chemistry, **17** (2007) 127.

Ruyu H.Y. *et al*., J. Materials Science, **39** (2004) 4377.

Rajeshwar A.W. *et al*., J. Electroanalytical Chemistry, **612** (2008) 112.